

The effect of post annealing on structure, microstructure and magnetic properties of thin Ni-Mn-Ga films

Anja Backen^{1,2,a}, Robert Niemann¹, Stefan Kaufmann¹, Jörg Buschbeck¹, Ludwig Schultz^{1,2} and Sebastian Fähler¹

¹ IFW Dresden, P.O. Box 270116, 01171 Dresden, Germany

² Dresden University of Technology, Departement of Mechanical Engineering, Institute of Materials Science, 01062 Dresden, Germany

Abstract. The magnetic shape memory (MSM) alloy Ni-Mn-Ga is an active material where large strains are obtained by magnetically induced reorientation (MIR) of martensitic variants. For the integration in microsystems, epitaxial thin films are in the centre of interest since the highest strains have only been obtained in single crystals. In order to minimize the technological effort, sputter deposition at low deposition temperatures is favoured. However, for obtaining high degree of order and thus a high Curie temperature, an additional post heat treatment at elevated temperatures is necessary. We report on the consequences of the post annealing process on thin epitaxial Ni-Mn-Ga films. In addition to increasing the Curie temperature, the annealed film shows a secondary Ni-rich Ni₃(Mn,Ga) phase. This phase has a well defined interface to the high temperature austenitic phase of Ni-Mn-Ga. Ni₃Ga is formed due to evaporation losses of Mn and Ga. The formation of those precipitates can be avoided by preparing thin Ni-Mn-Ga films directly at elevated temperatures.

1 Introduction

Ni₂MnGa is a magnetic shape memory (MSM) alloy which has been studied thoroughly in the last few years. Actuation can be achieved by reorientation of martensitic variants through twin boundary motion when applying a magnetic field. This effect was first observed in bulk samples [1]. High strains of up to 10 % have been obtained in single crystals [2]. Subsequently the integration of epitaxial films in microsystems is most interesting because it enables the use of the material directly without additional levers. Various groups have succeeded in preparing epitaxial Ni₂MnGa films on different substrates using sputter deposition [3, 4]. Compared to the first work on epitaxial growth where Molecular Beam Epitaxy (MBE) was used [5], sputtering is suitable for scaling up. However, epitaxial growth requires heating of the substrate to 350 °C and above. In order to decrease the technological effort, lower deposition temperatures are favourable. Apart from the integration in industrial processes, decreasing the deposition temperature has additional advantages like e.g. reduction of thermal stress during cooling and low evaporation losses of Mn and Ga. However, at too low temperatures the mobility of deposited atoms might be too low to obtain good crystallinity and a high degree of chemical order. Achieving a sufficient degree of order is crucial to obtain suitable structural and magnetic properties e.g. Curie temperatures (T_C) above room temperature [6]. An approach commonly used for bulk materials [7] as well as thin films [9] is subjecting the material to a post heat treatment at

^a e-mail: a.backen@ifw-dresden.de

elevated temperatures of typically 800°C [7]. In this paper, we report on the influence of a post annealing process on the structure, morphology and magnetic properties of Ni₂MnGa films. For this purpose, we deposited films at a low deposition temperature of 200°C and afterwards annealed them at 500°C in the deposition chamber. From comparing the as-deposited and annealed state we see severe challenges with respect to the suitability of post heat treatment of thin films for future applications.

2 Experimentals

Two Ni₂MnGa films with thicknesses of 500 nm were prepared using DC-Magnetron sputtering from a non-stoichiometric target Ni₅₀Mn₂₈Ga₂₂. Films were deposited on single crystal MgO(100) substrates covered by a buffer of 50 nm thickness. Ni-Mn-Ga films were deposited at $T_{dep} = 200$ °C with a power of 100 W. After deposition, one of the films was subjected to a post heat treatment at annealing temperature $T_{an} = 500$ °C for one hour. The annealing process took place in the deposition chamber at base pressure $p_B = 5 \cdot 10^{-9}$ mbar.

Ferromagnetic and martensitic transitions were investigated with temperature dependent magnetisation measurements. They were performed in the range of 50 K to 400 K in a low applied magnetic field of 10 mT using a Quantum Design PPMS with vibrating sample magnetometer (VSM). Film structure was determined by X-ray diffraction (XRD) methods using θ - 2θ -scans with Co-K α radiation and texture measurements with Cu-K α radiation in Phillips X'pert machines. Scanning Electron Microscopy (SEM) with a LEO Gemini 1530 as well as Atomic Force Microscopy (AFM) with a Digital Instruments Dimension 3100 in Tapping Mode were used to investigate the surface morphology of the films. The composition of the films was investigated with energy-dispersive X-ray spectroscopy (EDX) with an accuracy of about 0.5 at-% using a Ni₅₀Mn₂₅Ga₂₅ standard.

3 Results

Temperature dependent magnetisation measurements reveal that the Curie temperature T_C of the as-deposited film is 264 K and thus below room temperature (Figure 1 (a)). It suggests that a deposition temperature of 200 °C may not be enough to establish full L2₁ ordering of Ni₂MnGa [7]. To enhance the ordering and by this increase T_C , we performed post heat treatment of the as-deposited film. Indeed, by annealing the film at 500 °C for one hour, T_C is increased to 342 K (Figure 1 (a)). However after annealing we observe a two-step magnetisation curve, indicating the formation of a secondary phase which is ferromagnetic with T_C of about 220 K. There is no indication for a martensitic transition below T_C since this would typically result in a drop of magnetisation.

The θ - 2θ -scans of both films show a peak corresponding to the (400) reflection of non-modulated (NM) martensite (Figure 1 (b)). The intensities of those peaks however are very low. We performed θ - 2θ -scans in a Bragg-Brentano geometry where only variants with their axes parallel to the substrate normal can be observed. As described in a previous publication [8], martensitic transition results in a significant tilt of the unit cells away from the substrate normal. This tilt can be seen in pole figure measurements with 4-circle diffractometre. The four distinct peaks in the (400) pole figures of NM martensite (Figure 2) prove the epitaxial growth of Ni₂MnGa on the substrate-buffer-system. The epitaxial growth of Ni₂MnGa on MgO(100) substrates has been shown in previous studies [3]. The unit cell of austenitic Ni₂MnGa is rotated by 45° relative to the MgO cell with the epitaxial relation Ni₂MnGa(001)[110] || MgO(001)[100]. The lattice parameters of NM martensite obtained from measurements with the 4-circle diffractometre show no significant difference between the as-deposited ($a = 5.37$ Å; $c = 6.66$ Å) and the annealed state ($a = 5.39$ Å; $c = 6.68$ Å). Both films exhibit a c/a -ratio of 1.24 which agrees with bulk NM martensite. The (400) peaks in the as-deposited state are tilted by 4.5° from the substrate normal. In contrast to that the tilt in the annealed state is slightly smaller with 3°.

For the annealed film, the θ - 2θ -scan (Figure 1 (b)) furthermore shows an additional peak at $2\theta = 89.2^\circ$. This peak can be indexed with a (220) reflection of cubic Ni₃Ga. Pole figure

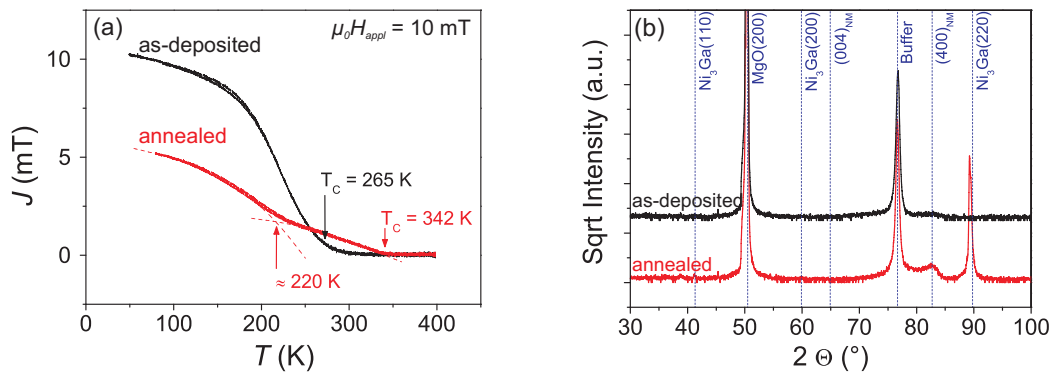


Fig. 1. (a) Post annealing increases the Curie temperature from 265 K in the as-deposited state (black) to 342 K (annealed film - red) as expected for a higher degree of ordering. The two step magnetisation curve after annealing indicates the formation of a second ferromagnetic phase. (b) The θ - 2θ -scans (measured in Bragg-Brentano geometry) reveal the existence of NM martensite in the as-deposited (black) and annealed (red) films. Annealing results in the formation of an additional phase which can be indexed as Ni_3Ga .

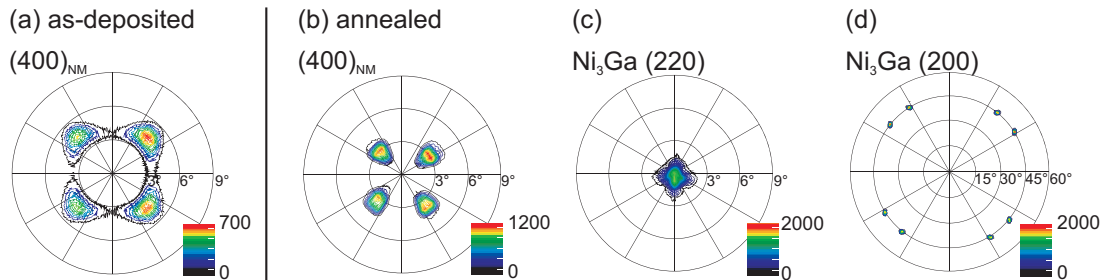


Fig. 2. The (400) pole figures of the NM martensite indicate that both as-deposited (a) and annealed films (b) are epitaxial. The (220) and (200) pole figures of the additional Ni_3Ga phase (c,d) show that phase is well oriented and exhibits some peak splitting. The two independent lattice spacings used for these measurements give a cubic phase with $a = 3.6 \text{ \AA}$.

measurements of Ni_3Ga (Figure 2(c,d)) confirm that it is highly textured and cubic with a lattice constant of $a = 3.6 \text{ \AA}$. Moreover, a peak splitting of 20° is observed in the (200) poles of Ni_3Ga (Figure 2(d)).

The as-deposited state has a flat, finely twinned surface (Figure 3(a)). Its composition $\text{Ni}_{54}\text{Mn}_{28}\text{Ga}_{18}$ slightly differs from the target composition ($\text{Ni}_{50}\text{Mn}_{28}\text{Ga}_{22}$) which can be explained with the evaporation of Mn and Ga during the deposition. This film composition gives an e/a ratio of 7.90 resulting in the formation of NM martensite [9,10]. After annealing, the SEM micrograph in Figure 3(b) shows precipitates on the film surface. These precipitates form lines with lengths of about $20 \mu\text{m}$ and widths of $2 \mu\text{m}$. According to the Fast Fourier Transformation (FFT) of the SEM image of the annealed film, the precipitates are rotated by about 6° relative to the [100] direction of MgO (Figure 3(c)). The height profiles obtained from AFM images (Figure 4) reveal that the precipitates have an increased height of about 60 nm whereas the area in between is finely twinned. EDX measurements were performed on two different spots on the annealed sample: the composition of the finely twinned area ($\text{Ni}_{54}\text{Mn}_{23}\text{Ga}_{23}$) is quite similar to the as-deposited film with slightly decreased Mn-content whereas line precipitates ($\text{Ni}_{67}\text{Mn}_{18}\text{Ga}_{15}$) exhibit a strongly increased Ni-content.

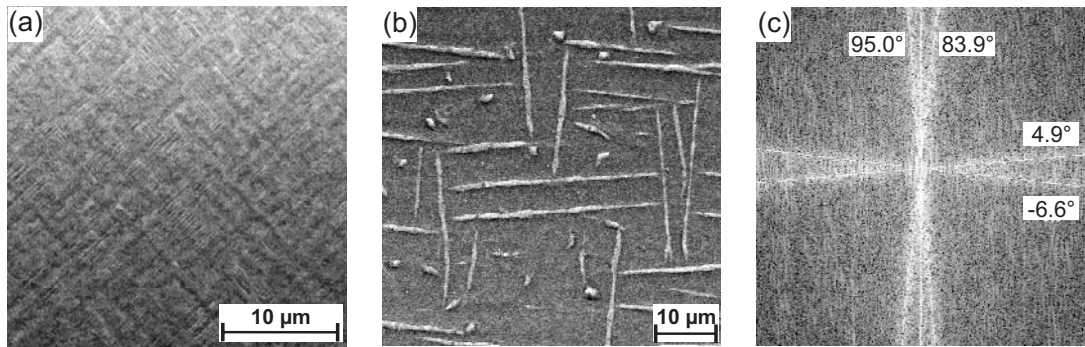


Fig. 3. The as-deposited film exhibits a smooth and finely twinned microstructure (a) whereas line precipitates are visible in the SEM micrograph after the post annealing process (b). The Fast Fourier Transformation of (b) reveals a well defined orientation of the precipitates which are rotated by about 6° from the [100] direction of MgO(c). The [100] direction of MgO is parallel to the edge of all figures (micrographs and polefigures)

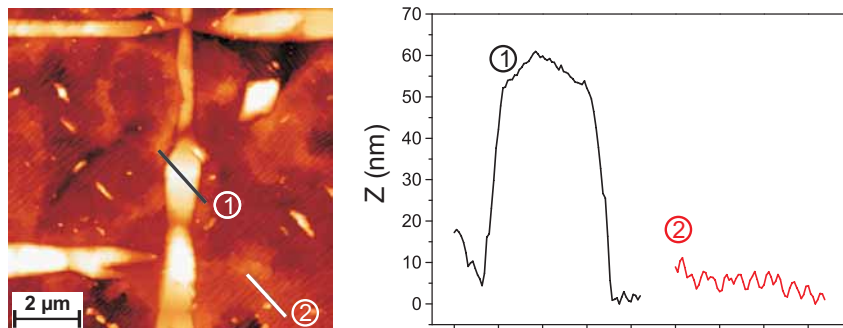


Fig. 4. The AFM image of the annealed sample displays that the line precipitates have an increased height of about 60 nm (Z-profile 1) compared to the finely twinned structure with heights of 2-4 nm and a periodicity of 150 nm in between (Z-profile 2).

4 Discussion

Annealing of a thin Ni_2MnGa film which was deposited at low deposition temperatures has several consequences. First, temperature dependent magnetisation measurements show a two-step curve with two different Curie temperatures of 220 K and 342 K. The formation of an additional Ni-rich phase Ni_3Ga explains this behaviour. Since Ni_3Ga is known to be paramagnetic at room temperature [12], we can assume that $T_C = 220$ K is related to Ni_3Ga . Consequently, T_C of Ni_2MnGa is increased from 265 K to 342 K by the post heat treatment we performed. It appears that a relatively low annealing temperature of 500°C is sufficient to enhance chemical ordering in the system. The annealing temperature we used is significantly lower than typical temperatures of about 800°C used for bulk samples. This is presumably due to the good chemical homogeneity obtained in sputter deposited films where the different types of atoms are distributed randomly over the substrate. However, even at this low temperature the losses of Mn and Ga are significant. The vapour pressures of Ni, Mn and Ga are strongly increasing with temperature [13]. Therefore the evaporation rates, which can be calculated using the Hertz-Knudsen equation [14], are increasing with temperature as well. Taken into account the annealing time of an hour, the thickness of evaporating material is shown in Figure 5. Since the evaporation rates of Mn and Ga are 10 orders of magnitude higher than Ni, the loss of Ni during annealing is negligible.

Evaporation of Mn and Ga during annealing leads to the formation of a secondary Ni-rich phase $\text{Ni}_3(\text{Mn,Ga})$. $\text{Ni}_3(\text{Mn,Ga})$ is isostructural with the cubic Ni_3Ga phase that is ordered in

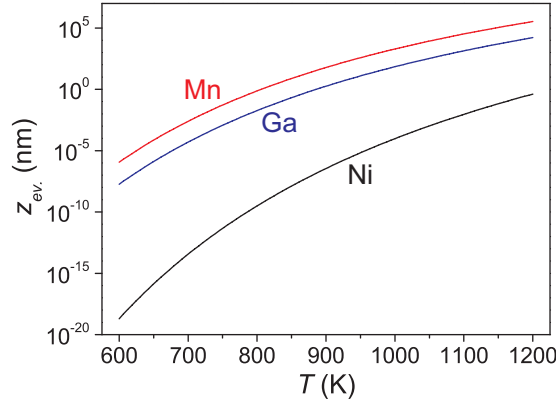


Fig. 5. Since the thicknesses of evaporating material of Mn and Ga are 10 orders of magnitudes higher than Ni, the loss of Ni due to evaporation can be neglected.

the L1₂ structure [15]. Our XRD measurements show that Ni₃Ga is well oriented with (220) plane parallel to the substrate surface. Furthermore we observe a peak splitting of the (200) poles (Figure 2(d)). At first glance, this might suggest that Ni₃Ga is martensitic since we observe similar splitting for martensitic Ni₂MnGa films [3]. However to our knowledge, there are no reports about a martensitic transition in the cubic Ni₃Ga phase. Furthermore we did not observe significant deviations from the cubic symmetry. Therefore this explanation for the peak splitting of Ni₃Ga (200) is very unlikely.

Another approach to explain the peak splitting may be a relation between Ni₃Ga and NM martensite. Ni₃Ga would form in the high temperature austenitic state. During cooling, austenite transforms to NM martensite which results in the tilt of the unit cells away from the substrate normal (Figure 2(a,b)). If the peak splitting of Ni₃Ga was a direct result of the martensitic transformation, the formed precipitates had to be rotated on top of the film. Since however the length of the precipitates of about 20 μm significantly exceeds the film thickness of 0.5 μm and by far the twinning periodicity of 150 nm, an extreme shear of the martensitic film would be required. Therefore this assumption can be excluded.

It is also very unlikely that the precipitates originate from a well defined interface to NM martensite since we can assume that austenite phase is stable at high temperatures [3].

In the following we will show that the texture of Ni₃Ga originates from the formation of a well defined interface between the high temperature austenitic phase of Ni₂MnGa and Ni₃Ga. We suggest that during heating NM martensite transforms to the cubic austenitic state. After this transition, a diffusion controlled evaporation of Mn and Ga presumably starts at defects on the sample surface. Once enough Mn and Ga have evaporated and the cubic Ni₃Ga phase becomes stable, an interface to the Ni₂MnGa austenite must form. By constructing pole figures of Ni₂MnGa and Ni₃Ga, it becomes obvious that Ni₂MnGa (220) and Ni₃Ga (111) are parallel to each other. We used the epitaxial relation of cubic austenitic Ni₂MnGa known from literature [3] and the measured orientation of Ni₃Ga (Ni₃Ga(220) || MgO(100) and Ni₃Ga(200) rotated by 55° from MgO[100]) for constructing the pole figures. Assuming that both phases are cubic, one can calculate lattice spacings of the parallel planes $d(hkl) = a/\sqrt{h^2 + k^2 + l^2}$ with a being lattice constant and h, k, l as Miller's indices. With $a_{Ni_2MnGa} = 5.83 \text{ \AA}$ [3] and the measured value $a_{Ni_3Ga} = 3.60 \text{ \AA}$ one obtains lattice spacing of $d(220)_{Ni_2MnGa} = 2.078 \text{ \AA}$ and $d(111)_{Ni_3Ga} = 2.061 \text{ \AA}$. The misfit between lattice spacings of those two planes is 0.8%. Both Ni₂MnGa (220) and Ni₃Ga (111) are the most densely packed planes within the corresponding crystal structure. Therefore it is very likely that those interfaces form once enough Mn and Ga have evaporated. The observed interface is not parallel to the substrate which is the common geometry for a depleted layer formed by evaporation. Hence we suggest that a favourable interface energy results in the formation of these precipitates.

The formation of the secondary phase can be avoided by depositing thin Ni₂MnGa films at elevated temperatures. Previous studies have shown, that even at temperatures of 350 °C ordered epitaxial films can be prepared on various substrates [3,16,17]. The deposited particles order at deposition temperatures that are less than half of the ordering temperature used for bulk. This is due to the different diffusion mechanisms. During deposition, ordering takes place via surface diffusion. In contrast to that, improving the order of deposited film requires diffusion within the film volume. Therefore however, vacancies have to be formed which only occurs at higher temperatures. Hence diffusion on a free surface is faster and needs less thermal activation than diffusion within the volume. Another advantage of depositing at slightly enhanced temperatures is that the loss of Mn and Ga due to evaporation can be compensated by adjusting the target composition and a homogeneous composition throughout the film can thus be obtained. However, even the cooling procedure directly after deposition seems to be crucial. When cooling slowly, it was observed that surface composition changes and that no martensitic transformation occurs at the surface [18].

5 Conclusion

We could show that in case of thin Ni₂MnGa films a post heat treatment at a temperature above the deposition temperature has two consequences. First, annealing increases the degree of chemical order of the system and thus the Curie temperature which allows to obtain the ferromagnetic phase at room temperature. Secondly, the formation of a secondary Ni-rich phase Ni₃(Mn,Ga) takes place. The secondary phase is not evenly distributed throughout the film but forms line precipitates with lengths of about 20 μm, widths of 2 μm and increased heights of 60 nm. The formation of those precipitates is presumably favoured by the evaporation of Mn and Ga during annealing and has a crystallogically well defined interface to the high temperature austenitic phase. Those precipitates can act as pinning centres for twin boundary motion and thus hinder the reorientation of martensitic variants. Depositing ordered, epitaxial films without any Ni-rich precipitates has been achieved at slightly increased deposition temperatures of 350 °C [3]. Due to the problems we encountered here, we can conclude that in case of thin films it is more favourable to enhance the temperature during preparation and avoid further post heat treatments under vacuum.

Acknowledgment

The authors would like to thank O. Heczko for valuable discussions. We graciously acknowledge funding by Deutsche Forschungsgemeinschaft (DFG) through the Priority Program "SPP1239" (www.magneticshape.de).

References

1. K. Ullakko et al., *Appl. Phys. Lett.* **69**, (1996) 1966-1968
2. A. Sozinov et al., *Appl. Phys. Lett.* **80**, (2002) 1746-1748
3. M. Thomas et al., *New Journ. Phys.* **10**, (2008) 023040
4. G. Jakob et al., *J. Mag. Mag. Mat* **310**, (2007) 2779
5. J.W. Dong et al., *Appl. Phys. Lett.* **75(10)**, (1999) 1443-1445
6. B.D. Cullity, C.D. Graham, *Introduction to Magnetic Materials* (Wiley, 2008) 145
7. P.J. Webster et al., *Phil. Mag. B* **49(3)**, (1984) 295
8. J. Buschbeck et al., *Acta Mat.* **57**, (2009) 2516-2526
9. V.A. Chernenko et al., *Smart Mat. Struct.* **14**, (2005) 245-252
10. A. Vasilev et al., *Journ. Mag. Mag. Mat* **197**, (1999) 837-839
11. V.A. Chernenko et al., *Phys. Rev. B* **57**, (1998) 2659
12. G.Y. Guo et al., *Journ. Mag. Mag. Mat.* **239**, (2002) 91-93
13. C.J. Smithells (Ed.), *Metals Reference Book* (Butterworths, 1983) 8-54, 8-55
14. R. Kelly et al., *Nucl. Inst. Meth. Phys. Res. B* **7/8**, (1985) 755

15. R. Ducher et al., *Intermetallics* **15**, (2007) 148-153
16. O. Heczko et al., *Appl. Phys. Lett.* **92**, (2008) 072502
17. M. Thomas et al., *Adv. Mater.* **21**, (2009) 1-4
18. P. Pörsch et al., *Appl. Phys. Lett.* **93**, (2008) 022501